Extended Abstracts of the 2012 International Conference on Solid State Devices and Materials, Kyoto, 2012, pp1011-1012

Effect of Geometrical Profile of Nanostructured Arrays on the Enhanced Optical Absorption of Silicon Thin-film Solar Cells

Yung-Chi Yao, Po-Wei Lu, and Ya-Ju Lee*

Institute of Electro-Optical Science and Technology, National Taiwan Normal University
88, Sec.4, Ting-Chou Road, Taipei 116, Taiwan
Phone: +886-2-7734-6733 E-mail: yajulee@ntnu.edu.tw

1. Introduction

Theoretical and experimental studies have indicated that nanostructured arrays which designed on Si solar cell can suppress optical reflections and promote the trapping of incident photons to improve the power conversion efficiency of Si solar cells [1, 2]. In this study, we use the finite-difference time-domain (FDTD) method to investigate the dependence of various nanostructured arrays on the enhanced optical absorption and power conversion efficiency of Si thin-film solar cells. By appropriately arranging the diameter and periodicity of the nanostructured array, the incident light that penetrates the crystal Si can be coupled into in-plane guided modes. As a result, an power conversion efficiency of η=17.4%, 18.8%, and 22.0% can be obtained for 2 μm-thick Si films of the nanorod, nanocone, and nanolens arrays, respectively.

2. Computational Simulations and Discussion

Figure 1(a) shows a schematic of nanorod, nanocone, and nanolens arrays which decorated on a crystal Si with a total thickness of 2 μm. Fig. 1(b) shows the corresponding profiles of the effective refractive indices (n_{eff}) along the z direction as diameter (D) increases from 100 nm to 300 nm .The n_{eff} of the nanostructured arrays governed by the Bruggeman model as follows [3]:

$$f_{Si}(z)\cdot\frac{n_{Si}^2-n_{eff}^2}{n_{Si}^2+2n_{eff}^2}+f_{air}(z)\cdot\frac{n_{air}^2-n_{eff}^2}{n_{air}^2+2n_{eff}^2}=0 \qquad (1)$$

where n_{Si} and n_{air} refer to the refractive indices of Si and air, respectively; $f_{Si}(z)$ and $f_{air}(z)$ are the weighting coefficients and $f_{Si}(z)+f_{air}(z)=1$. $f_{Si}(z)$ can be expressed as $f_{Si}(z)=\frac{\pi}{P^2}(\frac{D(z)}{2})^2$, where $D(z)$ is the diameter which varies along the z direction ($0\le z\le H$), and is defined for the different arrays as follows:

$$D(z)=2H, \text{ for nanorod} \qquad (2)$$

$$D(z)=2(H-z), \text{ for nanocone} \qquad (3)$$

$$D(z)=2\sqrt{H^2-z^2}, \text{ for nanolens} \qquad (4)$$

Fig. 2(a) shows a typical solar spectrum. Here, we mainly investigated incident wavelength of λ=320–1000 nm (blue dashed line). In Fig. 2(b)(c), the current density (J) versus the voltage (V) is expressed as follows [4]:

$$J(V)=\frac{q}{hc}\int_0^\infty \lambda\frac{dI}{d\lambda}A(\lambda)\,d\lambda-\frac{q(n^2+1)E_g^2kT}{4\pi\hbar^3c^2}e^{(\frac{eV-E_g}{kT})} \qquad (5)$$

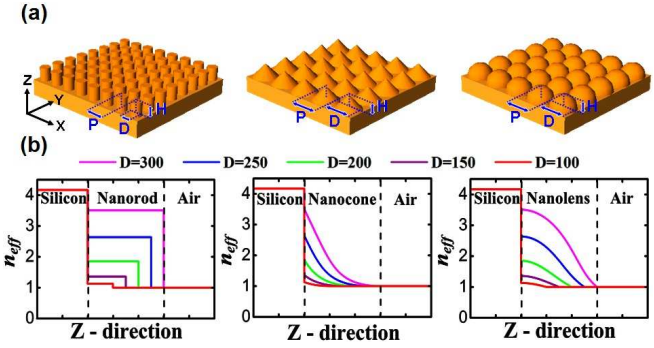

Fig. 1 (a) A schematic of nanorod, nanocone, and nanolens arrays successively. (b) The corresponding effective refractive index profiles along the z direction with in- creasing D(z).

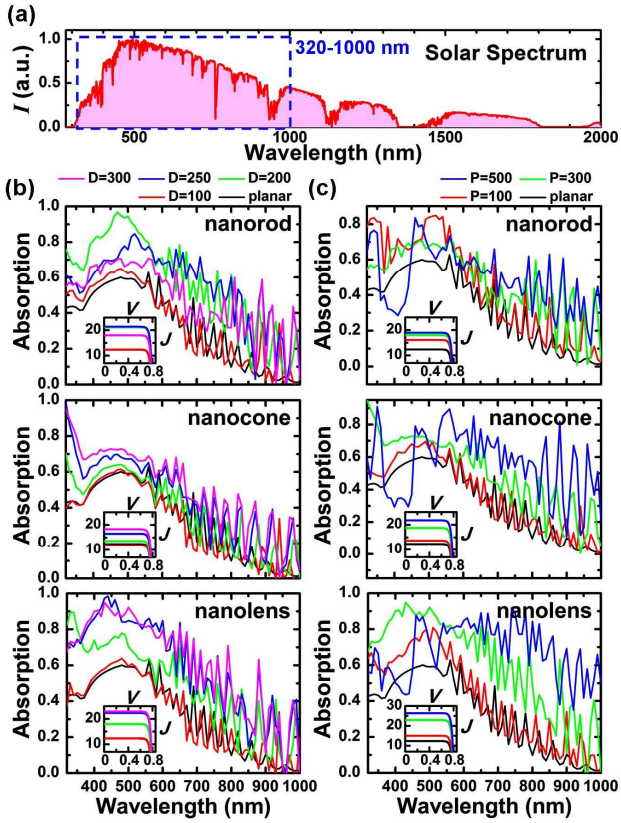

Fig. 2 (a) A.M. 1.5 solar spectrum. (b) The optical absorption spectra for different array diameters: D(z=0)=100, 200, 250, and 300 nm; Periodicity is set to P=300 nm. (c) The optical absorption spectra arranged in different periodicities (P=100, 300, and 500 nm). Insert: the corresponding J-V curves.

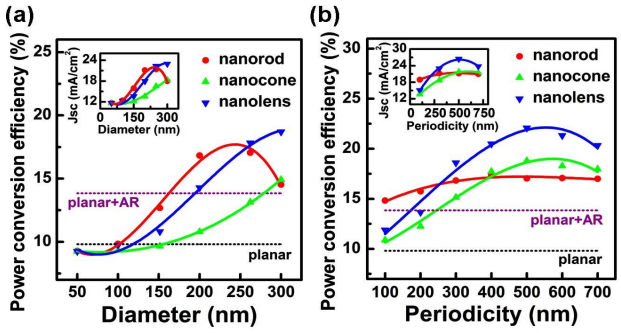

Fig. 3 The power conversion efficiency versus (a) the D and (b) the P of the nanostructured arrays. Planar Si thin-film solar cells with (η=13.8%) and without (η=9.8%) the AR layer serve as references. Insert: the short-circuit current density versus diameter and periodicity.

As shown in Fig. 2(b), for the nanolens arrays, the corresponding optical absorption spectra increase considerably because of their graded refractive index profile along the z direction with increasing D, which creates a broadband antireflection (AR) layer. In Fig. 2(c), when P is increased to P=300 nm, the optical absorption spectra for all are considerably enhanced, especially for the nanolens array. Most important, the optical absorption is shifted to the long wavelength regime as P increases. It indicates that the P of nanostructured arrays can considerably affect the enhanced optical absorption. Generally, the J-V curves for all of the nanostructured arrays shown in Fig. 2(b)(c) have a similar trend as the optical absorption spectra.

Fig. 3 plots the power conversion efficiency (η) versus (a) the D and (b) the P for all of the nanostructured arrays. By fixing P=300 nm [Fig. 3(a)], the η=17.0%, 14.9%, and 18.7% are obtained for the nanorod (D=250 nm), nanocone (D=300 nm), and nanolens (D=300 nm) arrays, respectively. While appropriately arranging the P of the nanostructured arrays [Fig. 3(b)], the η=17.4%, 18.8%, and 22.0% can be

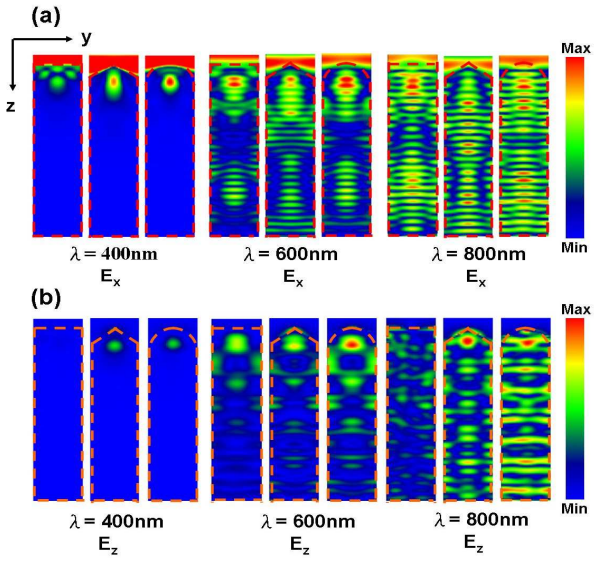

Fig. 4 The distributions of the simulated electric field of (a) E_x and (b) E_z in the nanostructured arrays for the incident wavelengths λ=400, 600, and 800 nm.

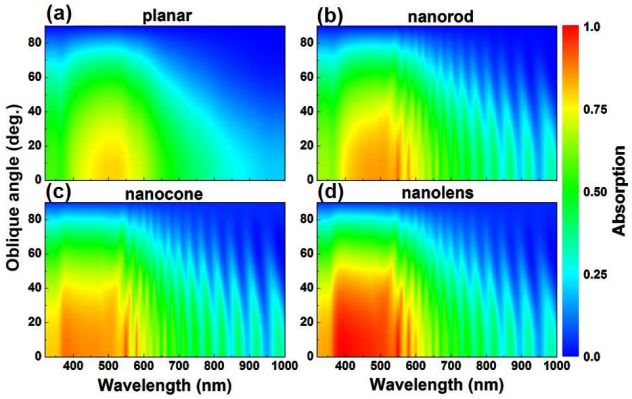

Fig. 5 The optical absorption $A(\theta, \lambda)$ as a function of the incident wavelength (λ) and the oblique angle (θ) for (a) the planar thin-film and (b) the nanorod, (c) nanocone, and (d) nanolens arrays.

obtained for the nanorod (P=400 nm), nanocone (P=600 nm), and nanolens (P=500 nm) arrays, respectively.

Fig. 4 shows the distribution of the simulated electric field for (a) $\vec{E}_x$ and (b) $\vec{E}_z$. In Fig. 4(b), particularly the nanolens array has the strongest integrated intensity of $\vec{E}_z$, can couple the incident light into optical modes ($\vec{k} = k_x\hat{i} + k_y\hat{j}$) guided within the crystal Si.

Fig. 5 shows the optical absorption $A(\theta, \lambda)$ as a function of the incident wavelength (λ) and the oblique angle (θ) for the optimized nanostructured arrays. The nanolens array shows the highest optical absorption, particularly for incident wavelength ranging from λ=350-600 nm. This wavelength range covers the highest energies from solar illumination [Fig. 2(a)].

3. Conclusions

In conclusion, we investigated the effect of the geometrical profile of nanostructured arrays on the performance of crystal Si thin-film solar cells. Of the three nanostructured arrays studied, the nanolens array offers excellent impedance matching between crystal Si and air through a continuous distribution of effective refractive indices, and it provides superior optical coupling with the incident light into in-plane guided modes. Besides, it also provides a promising way to enhanced absorption and power conversion efficiency of Si thin-film solar cells across a wide range of wavelengths and incident angles.

Acknowledgements

The authors gratefully acknowledge financial support from the National Science Council of Republic of China (ROC) in Taiwan (contract No. NSC–100–2112–M–003–006–MY3) and from the National Taiwan Normal University (award NTNU100-D-01).

References

[1] C. Lin, N. Huang, and M. L. Povinelli, Opt. Express **20** (2012) A125.

[2] Y.-C. Yao, M.-T. Tsai, H.-C. Hsu, L.-W. She, C.-M. Cheng, Y.-C. Chen, C.-J. Wu, and Y.-J. Lee, Opt. Express **20** (2012) 3479.

[3] D. E. Aspnes, Thin Solid Films **89** (1982) 249.

[4] P. Bermel, C. Luo, L. Zeng, L. C. Kimerling, and J. D. Joannopoulos, Opt. Express **15** (2007)16986.